On the number of views of polyhedral scenes

Boris Aronov[1], Hervé Brönnimann[1], Dan Halperin[2], and Robert Schiffenbauer[1]

[1] Polytechnic University, Brooklyn NY 11201, USA
{aronov,hbr,rschiff}@photon.poly.edu
[2] Tel-Aviv University, Tel-Aviv, Israel
halperin@math.tau.ac.il

Abstract. It is known that a scene consisting of k convex polyhedra of total complexity n has at most $O(n^4k^2)$ distinct orthographic views, and that the number of such views is $\Omega((nk^2+n^2)^2)$ in the worst case. The corresponding bounds for perspective views are $O(n^6k^3)$ and $\Omega((nk^2+n^2)^3)$, respectively. In this paper, we close these gaps by improving the lower bounds. We construct an example of a scene with $\Theta(n^4k^2)$ orthographic views, and another with $\Theta(n^6k^3)$ perspective views. Our construction can also be used to improve the known lower bounds for the number of silhouette views and for the number of distinct views from a viewpoint moving along a straight line.

1 Introduction

Aspect graphs have been studied in image analysis as a way to encode all topologically distinct views of a scene [2]. In this paper, we concentrate on simply bounding the *number* of such views, in the case where the scene consists of k disjoint convex polyhedra with total complexity (i.e., number of vertices, edges, and faces) n.

We distinguish between two different types of views: *orthographic* views correspond to locating the viewpoint on the plane at infinity and having all *lines of sight* parallel to the fixed viewing direction. *Perspective* views place the viewpoint anywhere in space, outside the objects of the scene. The *viewpoint space* is the space of all allowed placements of the viewpoint. It is (isomorphic to) the unit sphere of directions $\mathbb{S}^2$ in the orthographic model, and all of $\mathbb{R}^3$ (outside the polyhedra) in the perspective model.

In the *dynamic* viewpoint model, we consider a subset of the perspective model in which the viewpoint is restricted to move along a line (*linear motion*) or an algebraic curve (*algebraic motion*). In this model, the viewpoint space is a line in $\mathbb{R}^3$ for the linear motion model, and a curve in $\mathbb{R}^3$ for the algebraic motion model.

Topologically different views in the viewpoint space are separated by *critical events*: these occur at viewpoints where a visible vertex apparently lies on a visible edge (*EV event*) or when three visible edges appear to become concurrent (*EEE event*) [2]. Each event gives rise to a well-behaved curve on $\mathbb{S}^2$ (for the orthographic views) or surface in $\mathbb{R}^3$ (for the perspective views). If the total

number of vertices and edges of the scene is n, there can be at most $O(n^3)$ such events, and these critical events partition the viewpoint space into $O(n^6)$ regions in the orthographic model, and $O(n^9)$ regions in the perspective model. Matching lower bounds show that these bounds are worst-case tight for a general scene consisting of n triangles whether or not occlusions are considered [5, 2]. For axis-parallel objects in the orthographic model, the bound remains $\Omega(n^6)$ as demonstrated by Snoeyink [6].

The situation changes somewhat when we consider a scene consisting of k disjoint convex polyhedra having a total complexity of n, since occlusions no longer remain insignificant in the worst case: the fact that the n edges and vertices form the boundaries of only k convex objects limits the number of non-occluded EV or EEE events that can occur. No more than $O(n^2k)$ of them correspond to unoccluded events, and thus appear in the viewpoint space partition [3]. Hence the upper bounds on the number of distinct orthographic and perspective views become $O(n^4k^2)$ and $O(n^6k^3)$, respectively [3]. The best lower bounds are currently $\Omega((nk^2+n^2)^2)$ and $\Omega((nk^2+n^2)^3)$ [3].

An algebraic curve of constant degree may intersect each critical surface in at most a constant number of points, which implies an upper bound of $O(n^2k)$ on the number of distinct views in both the linear and algebraic motion models. The best lower bounds are currently $\Omega(nk+k^3)$ and $\Omega(nk^2+n^2)$, respectively [4].

Some authors have proposed a restricted notion of topologically different views, one that only takes into account *silhouette* critical events: these occur at viewpoints where a visible silhouette vertex apparently lies on a visible silhouette edge (*silhouette EV event*) or when three visible silhouette edges appear to become concurrent (*silhouette EEE event*) [2]. (Silhouette edges of a polyhedron are those that are incident to both a visible and an occluded facet from a given viewpoint, and a silhouette vertex is incident to a silhouette edge.) The number of distinct silhouette views in the linear motion model has been bounded by $O(nk^2)$, and by $O(n^2k)$ in the algebraic motion model. The best lower bounds are $\Omega(nk+k^3)$ and $\Omega(nk^2+n^2)$, respectively [4].

Our results. The main tool used by de Berg *et al.* [3] to argue their improved bounds is the assertion that no more than $O(n^2k)$ critical events can be met by a straight line, i.e., no more than $O(n^2k)$ distinct views can be observed by a viewpoint moving in a straight line. We argue that this bound is worst-case tight and construct a scene in which a particular straight-line motion of a viewpoint meets $\Theta(n^2k)$ EEE events at distinct points (and thus there are as many different views). This improves the lower bounds to a worst-case tight $\Theta(n^2k)$ for the number of views of k polyhedra having a total complexity of n, in both the linear and algebraic motion models.

Using this result, we show how to use two copies of our construction to force the existence of $\Omega(n^4k^2)$ distinct orthographic views. A similar technique using three copies shows a $\Omega(n^6k^3)$ lower bound on the number of distinct perspective views. Both bounds match the upper bounds of [3].

In the proceedings version, we had claimed that similar techniques can also be used to yield worst-case tight lower bounds of $\Omega(n^9)$ on the number of dis-

tinct perspective views of n axis-parallel objects. Unfortunately, this cannot be inferred by a direct application of our techniques, and the (conjectured) lower bound of $\Omega(n^9)$ remains open.

Finally, we can modify our construction slightly to prove the following lower bounds on the number of distinct silhouette views: $\Omega(nk^2)$ in the linear motion model, $\Omega(n^2k^4)$ in the orthographic model, and $\Omega(n^3k^6)$ in the perspective model. Unfortunately, we are unable to improve the existing lower bounds in the algebraic motion model.

Our paper is structured as follows. In the next section, we present the main construction. In Section 3, we show how this construction can be used to yield all the lower bounds on the number of views in the various models mentioned above. Finally, in Section 4, we argue by a perturbation argument that although our constructions exhibit degeneracies, our lower bounds are valid as well for non-degenerate constructions.

2 The main construction

We present a construction of a scene $\mathcal{C}$ with k polyhedra of total complexity n, that has at least $\Omega(n^2k)$ distinct views in the linear motion model (see figure 1). In addition to n and k, the scene that we construct depends on a scaling parameter t, $0 < t \leq 1$, and on $\varepsilon > 0$ that can be fixed as a function of n; t is required to produce scenes with many orthographic or perspective views and can be set to 1 for now.

More precisely, we prove the following.

Theorem 1. *As the viewpoint moves along the y-axis in the plane $z = +\infty$, it meets $\Omega(n^2k)$ critical surfaces of $\mathcal{C}$ at distinct points, and therefore observes at least as many distinct views of the scene.*

This bound is asymptotically the best possible [3].

Lines and directions not orthogonal to the z-direction and oriented downward can be parameterized by $(a, b, -1)$ [6]. The particular line at infinity used in the theorem corresponds to orthographic views in a direction $(0, b, -1)$, for $b \in \mathbb{R}$. Such directions are orthogonal to the x-direction. By making the viewpoint move along a line in $\mathbb{R}^3$ sufficiently far from $\mathcal{C}$, we can obtain a result similar to Theorem 1 about perspective views.

2.1 Description

Our construction consists of three distinct elements, the *drum*, the *needles* and the *fan*. The drum is a section of a nearly-flat horizontal prism; it has $\Theta(n)$ edges; we consider it completely flat in calculations and then choose its "curvature" small enough so that its slight non-flatness does not affect the construction. The fan is a convex polygon with $\Theta(n)$ edges that can be thickened to a proper convex polyhedron. The needles are a set of $\Theta(k)$ horizontal parallel lines that are eventually replaced by very thin and long tetrahedra.

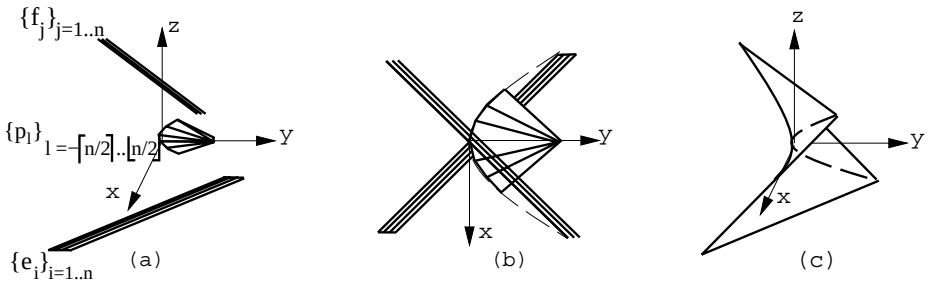

Fig. 1. The scene when $t = 1$: (a) a generic orthographic view of the scene, the drum is on the bottom, the fan in the middle, and the needles on the top; (b) another orthographic view from $z = \infty$; (c) the paraboloid and its parabolic section. When $t < 1$ the entire picture is compressed in the y-direction.

The intuition behind the construction is to place the elements so that each combination of a drum edge, a needle, and a fan edge yields an unoccluded EEE event. This can be done by placing them in an ε-neighborhood of the hyperbolic paraboloid $\Pi_0 : y = ztx$. We place the drum in the plane $z = -1$. The edges of the drum are parallel to the line $L_{-1} : y = -tx$, and at most ε away from L_{-1}. The needles are in the plane $z = 1$, parallel to and at most ε away from the line $L_1 : y = tx$. Both lines L_{-1} and L_1 belong to Π_0 (see figure 1c). The plane $x = z$ cuts Π_0 along the parabola $y = tx^2 = tz^2$; the fan is a polygon in this plane that "grazes" the paraboloid, its vertices are chosen on the parabola.

The exact coordinates of our construction are given in the table below.

	Neighborhood	Equation
Drum	L_{-1}	$e_i = \{x \in [-1,1],\ y = -t(x - \frac{i}{n}\varepsilon),\ z = -1\}$, for $i = 1, \ldots, n$
Needles	L_1	$f_j = \{x \in [-1,1],\ y = t(x + \frac{j}{k}\varepsilon),\ z = 1,$ for $j = 1, \ldots, n$
Fan	$\Pi_0 \cap \{x = z\}$	$[p_l, p_{l+1}]$ with $p_l = \left(\frac{l}{n}, t\left(\frac{l}{n}\right)^2, \frac{l}{n}\right)$, for $l = -\lceil \frac{n}{2} \rceil, \ldots, \lfloor \frac{n}{2} \rfloor$

Table 1. The elements of the construction. We fix $\varepsilon = \frac{1}{16n^2}$.

2.2 Analysis

We now proceed to prove Theorem 1. We show that each triple of edges e_i, f_j, $[p_l, p_{l+1}]$ gives rise to an unoccluded EEE event, for $i = 1, \ldots, n$, $j = 1, \ldots, k$, and $l = -\lceil \frac{n}{2} \rceil, \ldots, \lfloor \frac{n}{2} \rfloor$. We also show that the corresponding critical lines of sight include lines orthogonal to the x-direction.

In order to prove the latter statement, we introduce the surface $\Pi_{i,j}$ ruled by a family of lines orthogonal to the x-direction and passing through the drum edge e_i and the needle f_j. It is known that $\Pi_{i,j}$ is a hyperbolic paraboloid (e.g., [1,

Cor. 14.4.6]). The equation of $\Pi_{i,j}$, is of the form

$$\Pi_{i,j} \ : \ \pi_{i,j}(x,y,z) = 0,$$

where

$$\pi_{i,j}(x,y,z) = y - zt\left(x + \frac{\varepsilon}{2}\left(\frac{j}{k} - \frac{i}{n}\right)\right) - t\frac{\varepsilon}{2}\left(\frac{j}{k} + \frac{i}{n}\right). \tag{1}$$

Indeed, this equation is of the form $y = \alpha(x)z + \beta$ (implying that $\Pi_{i,j}$ contains a family of lines orthogonal to the x-direction); setting $z = -1$, we find that $\Pi_{i,j} \cap \{z = -1\}$ contains e_i, and similarly for $z = 1$, $\Pi_{i,j} \cap \{z = 1\}$ contains f_j.

Given a point $q = (x,y,z) \in \mathbb{R}^3$ not on the lines supporting e_i or f_j, there is a unique line passing through q and the lines supporting e_i and f_j; this line is the intersection of the planes aff$(q \cup e_i)$ and aff$(q \cup f_j)$ (see Figure 2). Let the direction of this line be $(a_{i,j}(q), b_{i,j}(q), -1)$. We will use the following property of $\Pi_{i,j}$. Since Π_{ij} contains all the lines that simultaneously touch the lines containing e_i, f_i and are orthogonal to the x-direction, $a_{i,j}(q) = 0$ if and only if q lies on Π_{ij}. In fact, the reader will verify easily (for example, by continuity of $a_{i,j}$) that if $\Pi^+_{i,j}$ stands for $\{(x,y,z) \in \mathbb{R}^3 \ : \ \pi_{i,j}(x,y,z) > 0\}$ and $\Pi^-_{i,j}$ for $\{(x,y,z) \in \mathbb{R}^3 \ : \ \pi_{i,j}(x,y,z) < 0\}$, then

$$\begin{cases} a_{i,j}(q) > 0 \text{ iff } q \in \Pi^+_{i,j}, \\ a_{i,j}(q) < 0 \text{ iff } q \in \Pi^-_{i,j}, \\ a_{i,j}(q) = 0 \text{ iff } q \in \Pi_{i,j}. \end{cases} \tag{2}$$

In view of (2), our goal can now be stated as follows: it suffices to prove that each segment $[p_l, p_{l+1}]$ intersects each hyperbolic paraboloid $\Pi_{i,j}$. Indeed, if q is in the intersection $[p_l, p_{l+1}] \cap \Pi_{i,j}$, considering the line of sight passing through q, e_i, and f_j, proves both that the triple e_i, f_j, and $[p_l, p_{l+1}]$ induces an EEE event, and (2) implies that the corresponding line of sight is orthogonal to the x-direction. Note that there can be at most two such intersections, because $\Pi_{i,j}$ is a hyperbolic paraboloid. Below, we prove the following: if q_l is the midpoint of p_l and p_{l+1}, then

$$\begin{cases} p_l, p_{l+1} \in \Pi^-_{i,j}, \\ q_l \in \Pi^+_{i,j}. \end{cases} \tag{3}$$

If (3) is true, $[p_l, q_l]$ must intersect $\Pi_{i,j}$ exactly once, and so must $[q_l, p_{l+1}]$. It should be clear also, that the corresponding lines of sight are ordered by slope in the yz-direction, as l takes on increasing values in $-\lceil \frac{n}{2} \rceil, \ldots, \lfloor \frac{n}{2} \rfloor$, and thus that the corresponding viewpoints on the y-axis in the plane $z = +\infty$ are all distinct.

Proof of (3). Let us begin by rewriting the equation of $\Pi_{i,j}$ as $\pi_{i,j}(x,y,z) = y - zt(x + \delta_{i,j}) - t\delta'_{i,j} = 0$, with $|\delta_{i,j}| \leq \delta'_{i,j} \leq \varepsilon$, and let us introduce the notation $x_l = \frac{l}{n}$. Note that $p_l = (x_l, t{x_l}^2, x_l)$. We compute

$$\begin{aligned} \pi_{i,j}(p_l) &= t{x_l}^2 - tx_l(x_l + \delta_{i,j}) - t\delta'_{i,j} \\ &= -t(x_l\delta_{i,j} + \delta'_{i,j}) < 0, \end{aligned}$$

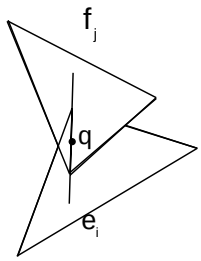

Fig. 2. There is a unique line passing through point q and tangent to e_i and f_j, and it is obtained as the intersection of the planes aff(q, e_i) and aff(q, f_j).

since $|x_l| < 1$ and $0 \leq |\delta_{i,j}| \leq \delta'_{i,j}$. Thus $p_l \in \Pi^-_{i,j}$, for $l = -\lceil \frac{n}{2} \rceil, \ldots, \lfloor \frac{n}{2} \rfloor$.

For q_l, we have $x(q_l) = z(q_l) = \frac{1}{2}(x_{l+1} + x_l)$, and $y(q_l) = \frac{t}{2}\left(x^2_{l+1} + x^2_l\right)$, therefore

$$\begin{aligned}
\pi_{i,j}(q_l) &= \frac{t}{2}\left(x^2_{l+1} + x^2_l\right) - \frac{t}{4}\left(x_{l+1} + x_l\right)^2 - \frac{t}{2}\left(x_{l+1} + x_l\right)\delta_{i,j} - t\delta'_{i,j} \\
&= \frac{t}{4}\left(x_{l+1} - x_l\right)^2 - \frac{t}{2}\left(x_{l+1} + x_l\right)\delta_{i,j} - t\delta'_{i,j} \\
&= \frac{t}{4n^2} - \frac{t}{2}\left(x_{l+1} + x_l\right)\delta_{i,j} - t\delta'_{i,j}
\end{aligned}$$

since $x_{l+1} - x_l = \frac{1}{n}$. Because $y(q_l) > 0$ and $|\delta_{i,j}| \leq \delta'_{i,j} \leq \varepsilon$, we have for our choice of $\varepsilon = \frac{1}{16n^2}$

$$\pi_{i,j}(q_l) > \frac{t}{4n^2} - 2t\varepsilon > 0.$$

Therefore, we have $q_l \in \Pi^+_{i,j}$. This completes the proof of (3), and by extension, of Theorem 1.

3 The lower bounds

We finish by indicating our various lower bound constructions. See Figure 4 for a pictorial explanation of our constructions. First we need a result about the critical curves and surfaces.

3.1 The critical curves and surfaces

Each orthographic viewpoint can be represented by a (oriented homogeneous) vector (a, b, c). Note that we are only concerned about the directions such that $c < 0$ here. As in [6], we treat these numbers as homogeneous coordinates, and the set of vectors such that $c < 0$ can be represented by the vector $(a, b, -1)$, or bijectively by a point (a, b) in the ab-plane at infinity. In that plane, the b-axis has equation $a = 0$.

The directions of the lines passing through e_i, f_j, and $[p_l, p_{l+1}]$ form a curve $\gamma_{i,j,l}$ in that plane. Each point of this curve corresponds to the point of contact $q_l(s) = (1-s)p_l + sp_{l+1}$ on $[p_l, p_{l+1}]$ (see Figure 2), with the endpoints of $\gamma_{i,j,l}$ corresponding to p_l and p_{l+1}. Thus the curve is naturally parameterized by $(a(s), b(s))$ with $s \in [0,1]$. Property (3) shows in fact that each such curve crosses the b-axis twice (see Figure 3a), once for some $s \in [0, \frac{1}{2}]$ and another for some $s \in [\frac{1}{2}, 1]$.[1] Let us consider only the portion $s \in [0, \frac{1}{2}]$ from now on.

In order to argue for complicated patterns of interaction later on (in Sections 3.2 and 3.3), we wish to find a rectangle $A \times B$ such that the critical curves completely traverse A in the a-direction, and remain constrained in an interval tB in the b-direction. We can compute an interval $A' = A'(n,k)$ such that $a(s)$ spans the entire interval A' as $s \in [0, \frac{1}{2}]$, for every choice of (i,j,l) in $I = \{1 \ldots n\} \times \{1 \ldots k\} \times \{-\lceil \frac{n}{2} \rceil + 1, \ldots, \lfloor \frac{n}{2} \rfloor\}$. Similarly, we can compute an interval $B = B(n,k)$ such that $b(s)$ remains always in B. Simply take:

$$
\begin{aligned}
A'_{\inf} &= \max_{(i,j,l) \in I} a(0) \; < 0, \\
A'_{\sup} &= \min_{(i,j,l) \in I} a(\frac{1}{2}) \; > 0, \\
B_{\inf} &= \min_{(i,j,l) \in I} \min_{s \in [0, \frac{1}{2}]} b(s), \\
B_{\sup} &= \max_{(i,j,l) \in I} \max_{s \in [0, \frac{1}{2}]} b(s),
\end{aligned}
$$

and let $A' = [A'_{\inf}, A'_{\sup}]$ and $B = [B_{\inf}, B_{\sup}]$. The sign conditions for A' follow from (2) and (3). Finally, we know that the intersections of the $\gamma_{i,j,l}$ with the b-axis are all distinct. We can therefore take a subinterval A of A' containing 0 such that the $\gamma_{i,j,l}$ do not pairwise intersect in the rectangle $A \times B$.

In summary, the critical curves completely traverse $A(n,k)$ in the a-direction, remain constrained in an interval $tB(n,k)$ in the b-direction, and do not pairwise intersect in the rectangle $A(n,k) \times tB(n,k)$. Thus, taking t small enough, the critical curves γ look as in Figure 3b, with the A-side much longer than the B-side.

Note also that seen from far away in the z-direction in the perspective model, the critical surfaces look like Figure 3c. Indeed, we can similarly select intervals $X(n,k)$, $Y(n,k)$ and $Z(n,k)$ of the same length such that the critical surfaces do not pairwise intersect in $X(n,k) \times tY(n,k) \times Z(n,k)$ and do not cross the top and bottom facets of the box. (The construction is straigthforward and omitted; it is possible to express X and Y as functions of A and B, and Z a subset of some interval $[z, +\infty)$ for some large enough z.) The situation is depicted on Figure 3b for the orthographic model, and 3c for the perspective model.

[1] In fact, these curves are the intersection of a hyperbolic paraboloid with a plane at infinity, and it can be shown that they are hyperbolas in that plane [6]. We will not need that characterization here.

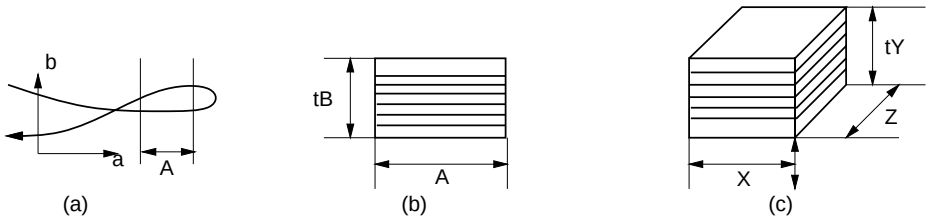

Fig. 3. (a) A critical curve and how to choose the interval A. (b) The critical curves in the orthographic model. (c) The critical surfaces when the viewpoint is sufficiently far away in the perspective model.

3.2 The number of views in the orthographic model

For the orthographic model, place two copies of the scene of Figure 1, one being the image of the other after a rotation of angle of $\pi/2$ about the z-axis and a suitable translation to avoid collisions (as in Figure 4a). By the results of the discussion in the previous section, in the viewpoint space, the critical curves overlap in a grid-like fashion. This method, which we call the *skew duplication* method, is already used in [3]. This proves that our scene yields $\Omega((n^2k)^2) = \Omega(n^4k^2)$ critical events.

3.3 The number of views in the perspective model

For the perspective model, place the view point at any vertex of a cube with sufficiently large side, and place three copies of the scene of Figure 1 at the three adjacent vertices, as in Figure 4b, with the orientation permuted in such a way that the critical surfaces will overlap in a grid-like fashion, yielding $\Omega((n^2k)^3) = \Omega(n^6k^3)$ critical events. This method, which we call the *skew triplication* method, is also already used in [3].

3.4 The number of silhouette views

For silhouette views, we modify the main construction by replacing the n edges of the drum by k needles e_i' in the neighborhood of L_{-1}, $i = 1, \ldots, k$. It should be clear that all the EEE events corresponding to e_i', f_j, and $[p_l, p_{l+1}]$ are silhouette events, and the same argument as above shows that indeed those $\Omega(nk^2)$ silhouette events are unoccluded, and can be observed as the viewpoint moves along the y-axis in the plane $z = +\infty$ (or a line in $\mathbb{R}^3$ sufficiently far from the scene, for perspective views). Thus the bound $\Omega(nk^2)$ for the maximum number of silhouette views in the linear motion model.

The bound extends naturally to $\Omega(n^2k^4)$ for the maximum number of silhouette views in the orthographic model, and to $\Omega(n^3k^6)$ for the maximum number of silhouette views in the perspective model, by using the same skew multiplication methods as in the previous two sections.

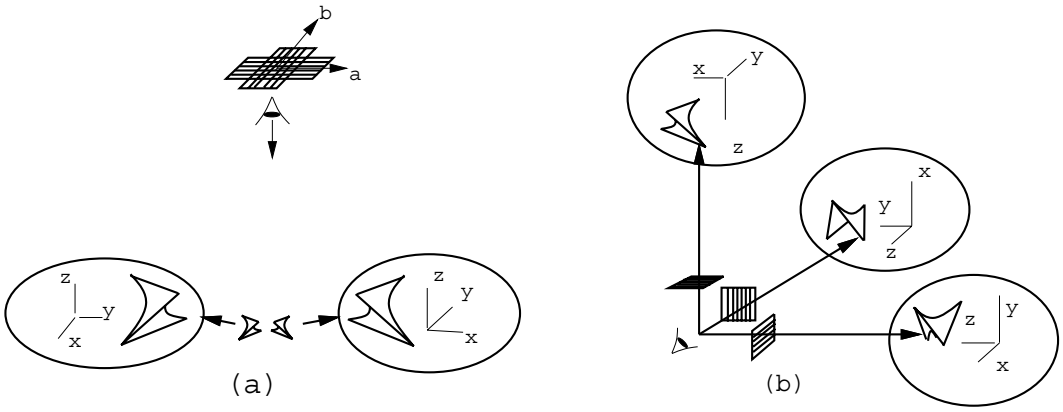

Fig. 4. How to arrange the scenes to obtain high complexity viewpoint space partitions in (a) the orthographic model, (b) the perspective model.

4 About degeneracies

There are three kinds of degeneracies arising in our construction: the facets of the drum are coplanar, the needles are segments and not polyhedra, and the fan is a polygon and not a polyhedron. We argue now that none of them affects our results.

To compensate for the fact that the facets of the drum are coplanar, we can introduce a perturbation to put these edges in a convex position, depending on a small positive parameter η_1, by putting edge e_i in the plane $z = -1 - \eta_1 i^2$.

The needles are segments, but we can replace the x-smaller endpoint of each needle by a small triangle containing the endpoint, whose sides are smaller than a parameter $\eta_2 n$. A needle is thus a very long and thin tetrahedron. By choosing an appropriate orientation of these tetrahedra, we can make f_j visible on the contour when viewed from all the (near-vertical) directions of interest in this paper; take the vertices of the triangle at the basis of f_j to be $f_j(-1)$, $f_j(-1) + \eta_2 j \boldsymbol{e_y}$, and $f_j(-1) + \eta_2 j \boldsymbol{e_y} + {\eta_2}^2 j^2 \boldsymbol{e_z}$.

As presented, the fan is a polygon rather than a polyhedron. We can make the fan into a convex polyhedron with non-empty interior by taking the convex hull of the p_l's with an edge of length η_3, whose endpoints are $(0, 1, -\eta_3)$ and $(0, 1, \eta_3)$.

We argue that the introduction of the η's does not affect the veracity of the proof. This can be formally checked by the following approach: check that neither η_1 nor η_2 nor η_3 appear in the asymptotically dominant term of any quantity on which we assert the sign (positive or negative; we do not rely on any quantity to be exactly 0), such as in the grazing property (2), or in the existence of $A(n, k)$, (n, k) and $B(n, k)$ above. Therefore the bounds remain valid for sufficiently small values of η_1, η_2, and η_3.

References

1. M. Berger. *Geometry (vols. 1-2)*. Springer-Verlag, 1987.
2. K. W. Bowyer and C. R. Dyer. Aspect graphs: An introduction and survey of recent results. *Int. J. of Imaging Systems and Technology*, 2:315–328, 1990.
3. M. de Berg, D. Halperin, M. Overmars, and M. van Kreveld. Sparse arrangements and the number of views of polyhedral scenes. *Internat. J. Comput. Geom. Appl.*, 7:175–195, 1997.
4. A. Efrat, L. J. Guibas, O. A. Hall-Holt, and L. Zhang. On incremental rendering of silhouette maps of a polyhedral scene. In *Proc. 13th ACM-SIAM Sympos. Discrete Algorithms*, 2000.
5. H. Plantinga and C. R. Dyer. Visibility, occlusion, and the aspect graph. *Internat. J. Comput. Vision*, 5(2):137–160, 1990.
6. J. Snoeyink. The number of views of axis-parallel objects. *Algorithms Rev.*, 2:27–32, 1991.